JOC*Article*

Determination of Molecular Structure Using Vibrational Circular Dichroism Spectroscopy: The Keto-lactone Product of Baeyer−Villiger Oxidation of (+)-(1*R*,5*S*)-Bicyclo[3.3.1]nonane-2,7-dione

P. J. Stephens,* D. M. McCann, F. J. Devlin, and T. C. Flood

Department of Chemistry, University of Southern California, Los Angeles, California 90089-0482

E. Butkus and S. Stončius

Department of Organic Chemistry, Vilnius University, Naugarduko 24, LT-03225 Vilnius, Lithuania

J. R. Cheeseman

Gaussian Inc., 340 Quinnipiac Street, Building 40, Wallingford, Connecticut 06492-4050

pstephen@usc.edu

Received November 24, 2004

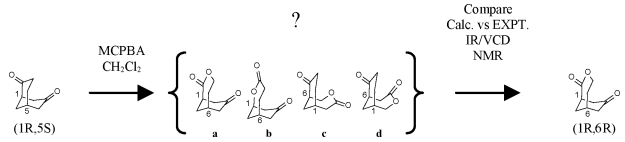

The Baeyer−Villiger oxidation of (+)-(1*R*,5*S*)-bicyclo[3.3.1]nonane-2,7-dione, **1**, can lead to four keto-lactone products, **2a**−**d**. A single isomer is obtained experimentally. We have used IR and VCD spectroscopies to identify the structure of this product. DFT calculations of the IR and VCD spectra of **2a**−**d** show unambiguously that the experimental product is (+)-(1*R*,6*R*)-**2a**, and not the expected product **2b**. NMR studies, including comparison of DFT and experimental ^{1}H and ^{13}C spectra, support this conclusion. This work provides the first example of the use of VCD spectroscopy to discriminate between structural isomers of a chiral molecule. The specific rotation of (+)-(1*R*,6*R*)-**2a**, predicted using TDDFT methods, is negative demonstrating that absolute configurations determined from TDDFT calculations of specific rotations are not 100% reliable.

Introduction

The vibrational circular dichroism (VCD) spectrum of a chiral molecule[1] is a sensitive function of its structure. As a result of the application of density functional theory (DFT) to the prediction of VCD spectra,[2] utilization of VCD spectroscopy for molecular structure determination has increased dramatically in recent years.[1c−e,3] However, applications have been limited to conformational analysis of flexible molecules[3a,b,d,j] and to absolute configuration (AC) determination.[3c,e−i,k] To date, VCD has not been used to differentiate structural isomers. Here, we report the first such application of VCD spectroscopy. We examine the structure of the keto-lactone product of Baeyer−Villiger oxidation of (+)-(1*R*,5*S*)-bicyclo[3.3.1]nonane-2,7-dione, (+)-(1*R*,5*S*)-**1**.

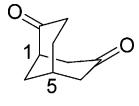

(1R,5S)-**1**

Four keto-lactone products are possible: (1*R*,6*R*)-3-oxabicyclo[4.3.1]decane-2,8-dione, **2a**; (1*R*,6*S*)-2-oxabicyclo-

(1) (a) Stephens, P. J.; Lowe, M. A. *Annu. Rev. Phys. Chem.* **1985**, *36*, 213−241. (b) Stephens, P. J. In *Encyclopedia of Spectroscopy and Spectrometry*; Lindon, J. C., Tranter, G. E., Holmes, J. L., Eds.; Academic: London, 2000; pp 2415−2421. (c) Stephens, P. J.; Devlin, F. J. *Chirality* **2000**, *12*, 172−179. (d) Stephens, P. J.; Devlin, F. J.; Aamouche, A. In *Chirality: Physical Chemistry*; Hicks, J. M., Ed.; ACS Symposium Series 810; American Chemical Society: Washington, DC, 2002; Chapter 2, pp 18−33. (e) Stephens, P. J. In *Computational Medicinal Chemistry for Drug Discovery*; Bultinck, P., de Winter, H., Langenaecker, W., Tollenaere, J., Eds.; Dekker: New York, 2003; Vol. 26, pp 699−725.

(2) (a) Cheeseman, J. R.; Frisch, M. J.; Devlin, F. J.; Stephens, P. J. *Chem. Phys. Lett.* **1996**, *252*, 211−220. (b) Stephens, P. J.; Ashvar, C. S.; Devlin, F. J.; Cheeseman, J. R.; Frisch, M. J. *Mol. Phys.* **1996**, *89*, 579−594. (c) Devlin, F. J.; Stephens, P. J.; Cheeseman, J. R.; Frisch, M. J. *J. Phys. Chem.* **1997**, *101*, 6322−6333. (d) Devlin, F. J.; Stephens, P. J.; Cheeseman, J. R.; Frisch, M. J. *J. Phys. Chem. A* **1997**, *101*, 9912−9924.

10.1021/jo047906y CCC: $30.25
Published on Web 04/16/2005

[4.3.1]decane-3,8-dione, **2b**; (1*R*,6*S*)-3-oxabicyclo[4.3.1]-decane-4,9-dione, **2c**; and (1*S*,6*R*)-3-oxabicyclo[4.3.1]-decane-4,7-dione, **2d**.

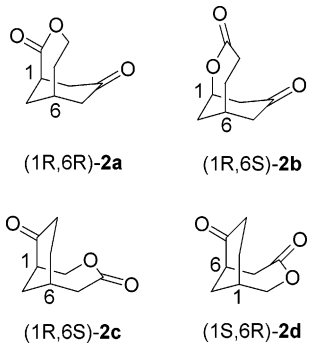

Butkus and Stončius isolated a single keto-lactone product from the Baeyer−Villiger oxidation of (±)-**1** using meta-chloro-peroxybenzoic acid (MCPBA).[4] On the basis of the proton NMR spectrum it was identified as (±)-**2a**. Subsequently, Stončius, Berg, and Butkus reported the oxidation of (+)-(1*R*,5*S*)-**1**.[5] The specific rotation, $[\alpha]_{546}$, of the product was positive, and hence the AC of **2a** was assigned as (1*R*,6*R*)-(+)/(1*S*,6*S*)-(−).

The conclusions of Butkus and co-workers were called into question by calculations of the specific rotation of **2a** using the time-dependent density functional theory/gauge-invariant (including) atomic orbital (TDDFT/GIAO) methodology[6] which predict the AC to be (1*R*,6*R*)-(−)/(1*S*,6*S*)-(+) (vide infra). The AC, (1*R*,5*S*)-(+)/(1*S*,5*R*)-(−), of the precursor, **1**, has been firmly established,[7] and an error in the AC of **1** is very unlikely to be responsible for the discrepancy. We have therefore investigated the possibility that the oxidation product might in fact be an isomer of **2a**: i.e., **2b**, **2c**, or **2d**. A further reason to explore this possibility is provided by the standard mechanism of the Baeyer−Villiger reaction which predicts a product whose structure depends on the migratory aptitudes of the groups adjacent to the ketone group.[8] In the case of **1**, the normally greater migratory aptitude of tertiary alkyl over secondary alkyl groups leads to the expectation that **2b** should be the product. In order to remove the uncertainty in the structure of the Baeyer−Villiger oxidation product of (+)-**1**, we have measured its IR and VCD spectra. Comparison to DFT predictions of the IR and VCD spectra of the four possible products, **2a**−**d**, then unambiguously defines the isomer obtained experimentally.

In addition, we have reinvestigated the NMR of the Baeyer−Villiger oxidation product of **1**, both experimentally, using 2D NMR methods, and theoretically, using DFT methodologies for calculating nuclear shielding constants/chemical shifts[9] and nuclear spin−spin coupling constants[10] and, thence, the ^{1}H and ^{13}C spectra of **2a**−**d**. The results obtained are fully consistent with the conclusions arrived at using IR and VCD spectroscopies.

Methods

Synthesis. (+)-(1*S*,5*S*)-Bicyclo[3.3.1]nonane-2,6-dione, (+)-**3**, was obtained via baker's yeast resolution of (±)-**3**, as described previously:[11] ee 99% (GC), $[\alpha]_D$ = 207 (*c* 0.27, CH_3OH). (+)-**3** was converted to (+)-(1*R*,5*S*)-bicyclo[3.3.1]-nonane-2,7-dione, (+)-**1**, via the synthetic route described previously:[11b] ee 98% (GC), $[\alpha]_{546}$ = 193 (c 0.675, $CHCl_3$). (+)-**1** was converted to (+)-**2** following the procedure of Stončius et al.[5] A 1.5-fold molar excess of MCPBA (75%) and $NaHCO_3$ (~4-fold molar excess to MCPBA) was added to a stirred solution of (+)-**1** (60 mg, 0.40 mmol) in dichloromethane (5.0 mL). The reaction mixture was stirred at room temperature for 1.5 h. Solid sodium sulfite (0.1 g) and water (0.1 mL) were added and stirred for 0.5 h. The mixture was filtered through Na_2SO_4, dried over Na_2SO_4, and evaporated. The solid residue was purified by flash chromatography (4:6 heptane/ethyl acetate, R_f 0.28) to give keto lactone (+)-**2**: yield 10 mg (15%), mp 110−111 °C. (±)-**2** was synthesized using the same method.

It should be noted that the isolated yield of **2** was rather low due to the hydrolysis of the latter during the reaction and that in addition, **2** is unstable in alcoholic solutions.

Conformational Analysis. The conformations of **2a**−**d** were identified using the MMFF94 Monte Carlo methodology of SPARTAN 02.[12] All stable conformations found were further optimized, and their vibrational frequencies and free energies calculated at the B3LYP/6-31G* level using GAUSSIAN 98/03.[13] For the lowest free energy conformations of **2a**−**d**, further optimizations, vibrational frequency calculations, and free energy calculations were carried out at the B3LYP/TZ2P and B3PW91/TZ2P levels using GAUSSIAN 98/03.

IR and VCD. The IR and VCD spectra of a 0.061 M $CHCl_3$ solution of (+)-**2** were measured using Nicolet MX-1 and Bomem/BioTools Chiral IR spectrometers, respectively. The Chiral IR spectrometer is equipped with a "Dual Photoelastic Modulator" accessory.[14] The baselines for the IR and VCD

(3) For examples, see: (a) Ashvar, C. S.; Devlin, F. J.; Stephens, P. J. *J. Am. Chem. Soc.* **1999**, *121*, 2836−2849. (b) Devlin, F. J.; Stephens, P. J. *J. Am. Chem. Soc.* **1999**, *121*, 7413−7414. (c) Aamouche, A.; Devlin, F. J.; Stephens, P. J. *J. Am. Chem. Soc.* **2000**, *122*, 2346−2354. (d) Aamouche, A.; Devlin, F. J.; Stephens, P. J. *J. Am. Chem. Soc.* **2000**, *122*, 7358−7367. (e) Aamouche, A.; Devlin, F. J.; Stephens, P. J.; Drabowicz, J.; Bujnicki, B.; Mikolajczyk, M. *Chem.−Eur. J.* **2000**, *6*, 4479−4486. (f) Stephens, P. J.; Aamouche, A.; Devlin, F. J.; Superchi, S.; Donnoli, M. I.; Rosini, C. *J. Org. Chem.* **2001**, *66*, 3671−3677. (g) Devlin, F. J.; Stephens, P. J.; Scafato, P.; Superchi, S.; Rosini, C. *Tetrahedron: Asymmetry* **2001**, *12*, 1551−1558. (h) Devlin, F. J.; Stephens, P. J.; Scafato, P.; Superchi, S.; Rosini, C. *Chirality* **2002**, *14*, 400−406. (i) Devlin, F. J.; Stephens, P. J.; Oesterle, C.; Wiberg, K. B.; Cheeseman, J. R.; Frisch, M. J. *J. Org. Chem.* **2002**, *67*, 8090−8096. (j) Devlin, F. J.; Stephens, P. J.; Scafato, P.; Superchi, S.; Rosini, C. *J. Phys. Chem. A* **2002**, *106*, 10510−10524. (k) Cerè, V.; Peri, F.; Pollicino, S.; Ricci, A.; Devlin, F. J.; Stephens, P. J.; Gasparrini, F.; Rompietti, R.; Villani, C. *J. Org. Chem.* **2005**, *70*, 664−669.

(4) Butkus, E.; Stončius, S. *J. Chem. Soc., Perkin Trans. 1* **2001**, 1885−1888.

(5) Stončius, S.; Berg, V.; Butkus, E. *Tetrahedron: Asymmetry* **2004**, *15*, 2405−2413.

(6) (a) Stephens, P. J.; Devlin, F. J.; Cheeseman, J. R.; Frisch, M. J. *J. Phys. Chem. A* **2001**, *105*, 5356−5371. (b) Stephens, P. J.; Devlin, F. J.; Cheeseman, J. R.; Frisch, M. J.; Rosini, C. *Org. Lett.* **2002**, *4*, 4595−4598. (c) Stephens, P. J.; Devlin, F. J.; Cheeseman, J. R.; Frisch, M. J.; Bortolini, O.; Besse, P. *Chirality* **2003**, *15*, S57−S64.

(7) Stephens, P. J.; McCann, D. M.; Butkus, E.; Stončius, S.; Cheeseman, J. R.; Frisch, M. J. *J. Org. Chem.* **2004**, *69*, 1948−1958.

(8) (a) Krow, G. R. *Tetrahedron* **1981**, *37*, 2697−2946. (b) Lowry, T. H.; Richardson, K. S. *Mechanism and Theory in Organic Chemistry*, 3rd ed.; Harper & Row: New York, 1987; pp 501−504.

(9) Cheeseman, J. R.; Trucks, G. W.; Keith, T. A.; Frisch, M. J. *J. Chem. Phys.* **1996**, *104*, 5497−5509.

(10) Peralta, J. E.; Scuseria, G. E.; Cheeseman, J. R.; Frisch, M. J. *Chem. Phys. Lett.* **2003**, *375*, 452−458.

(11) (a) Hoffman, G.; Wiartalla, R. *Tetrahedron Lett.* **1982**, *23*, 3887−3888. (b) Butkus, E.; Berg, U.; Zilinskas, A.; Kubilius, R.; Stončius, S. *Tetrahedron: Asymmetry* **2000**, *11*, 3053−3057. (c) Butkus, E.; Stončius, S.; Zilinskas, A. *Chirality* **2001**, *13*, 694−698.

(12) *SPARTAN 02*; Wave function Inc.: Irvine, CA, www.wavefunction.com.

(13) *GAUSSIAN 98/03*; Gaussian Inc.: Wallingford, CT, www.Gaussian.com.

(14) Nafie, L. A. *Appl. Spectrosc.* **2000**, *54*, 1634−1645.

spectra were provided by $CHCl_3$ and a 0.063 M $CHCl_3$ solution of (±)-**2**, respectively. IR and VCD resolutions were 1 and 4 cm^{-1}, respectively. VCD scan times were 1 h. KBr cells with path lengths of 597 and 239 μm were used.

Harmonic vibrational frequencies, dipole strengths, and rotational strengths of the lowest free energy conformations of **2a**−**d** were calculated using DFT[2] at the B3LYP/TZ2P and B3PW91/TZ2P levels via GAUSSIAN 98/03. IR and VCD spectra were obtained thence using Lorentzian band shapes[2c,d] with $\gamma = 4.0$ cm^{-1}.

NMR. NMR spectra of (±)-**2** were acquired in $CDCl_3$ solution using an inverse probe with a pulsed *z*-gradient. Standard software pulse sequences were used for all acquisitions, and all parameters employed were standard.

^1H and ^{13}C NMR chemical shifts and indirect NMR spin−spin coupling constants for **2a**−**d** were calculated using GAUSSIAN 03. ^1H and ^{13}C NMR chemical shifts, with respect to TMS, were calculated using GIAOs at the B3LYP/aug-cc-pVDZ level. The NMR indirect spin−spin coupling constant consists of four terms: the Fermi contact (FC), the spin dipolar (SD), the paramagnetic spin−orbit (PSO), and the diamagnetic spin−orbit (DSO). The FC term is usually the dominant contribution and is also the most sensitive to the quality of the basis set requiring large uncontracted basis sets augmented with tight *s* functions.[10,15−17] The FC contributions were calculated using B3LYP and a fully uncontracted aug-cc-pVDZ basis set augmented with tight *s* functions taken from the large uncontracted universal Gaussian basis set (UGBS) of de Castro and Jorge.[18] The first six UGBS *s* functions were used for carbon and oxygen, and the first 10 UGBS *s* functions were used for hydrogen. The SD, PSO, and DSO contributions, which are less basis set sensitive than the FC contribution, were calculated at the B3LYP/aug-cc-pVDZ level. ^1H and ^{13}C spectra were obtained from calculated chemical shifts and spin−spin coupling constants using the NUTS program.[19]

OR and ECD. Specific rotations, $[\alpha]_\nu$, of the lowest free energy conformations of **2a**−**d** were calculated using the TDDFT/GIAO methodology[6] implemented in GAUSSIAN 03. Electronic excitation energies and rotational strengths were calculated using the TDDFT method (without GIAOs)[7,20] in GAUSSIAN 03. Both length and velocity representations of rotational strengths were calculated.

Results

Conformational Analysis. Conformational analysis of the four isomers of **2**, **2a**−**d**, has been carried out using the following protocol. First, Monte Carlo conformational searching is carried out using the MMFF94 molecular mechanics force field. Second, the MMFF94 conformations obtained are further optimized using DFT at the B3LYP/6-31G* level. Third, B3LYP/6-31G* vibrational frequencies are calculated and, thence, the relative free energies of the B3LYP/6-31G* conformations obtained. The MMFF94 and B3LYP/6-31G* relative energies and the B3LYP/6-31G* relative free energies of the conformations of **2a**−**d** found using this protocol are given in Table 1. In each case, the chair−chair (CC) conformation is lowest in both energy and free energy, and the other conformations are all >2 kcal mol^{-1} higher in free energy. Accordingly, at room temperature, equilibrium conformational mixtures of **2a**−**d** are predicted to contain essentially only one conformation, i.e., all four isomers are effectively rigid molecules.

TABLE 1. Conformational Analysis of 2a−d

		MMFF94	B3LYP/6-31G*		
	confn.[a]	ΔE^b	ΔE^b	ΔG^b	P (%)[c]
2a	CC	0.00	0.00	0.00	98.9
	CC	4.43			
	CB	3.77	3.02	2.80	0.9
	CB	4.92			
	CtC	4.99	3.78	3.70	0.2
	CtC	8.47			
	tBtB	7.10	5.69	5.15	0.0
	tBtB	5.57	5.41	5.25	0.0
	tBtB	7.27	5.05	5.36	0.0
2b	CC	0.00	0.00	0.00	99.5
	BC	3.11			
	CB	2.65	3.22	2.72	0.4
	tBtB	5.40	4.74	4.77	0.0
	tBtB	5.85	5.61	5.05	0.0
	tBtB	8.00	5.85	5.71	0.0
	tBtC	8.31			
2c	CC	0.00	0.00	0.00	95.6
	BC	2.61	2.28	2.16	2.5
	CB	0.75	1.99	2.41	1.6
	CtB	1.91	3.96	3.88	0.1
	tBtB	2.33	4.93	4.68	0.0
	CtC	1.77	5.01	4.68	0.0
	BtC	4.20	6.08	6.15	0.0
2d	CC	0.00	0.00	0.00	97.0
	CB	1.87	1.57	2.06	3.0
	CtB	1.08	3.43	2.90	0.7
	CtB	4.14	4.65	4.63	0.0

[a] C = chair, B = boat, tC = twist-chair, and tB = twist-boat. The first and second labels apply to the 6- and 7-membered rings, respectively. [b] ΔE and ΔG in kcal mol^{-1}. [c] Populations calculated using ΔG values at 298 K.

TABLE 2. Relative Energies and Free Energies of the CC Conformations of 2a−d

	B3LYP/6-31G*		B3LYP/TZ2P		B3PW91/TZ2P	
	ΔE^a	ΔG^a	ΔE^a	ΔG^a	ΔE^a	ΔG^a
2a	2.41	2.58	2.35	2.63	2.28	2.67
2b	0.00	0.00	0.00	0.00	0.00	0.00
2c	1.63	2.07	1.76	2.34	1.70	2.33
2d	2.03	2.44	2.12	2.66	2.09	2.71

[a] ΔE and ΔG in kcal mol^{-1}.

Further optimizations of the geometries of the CC conformations of **2a**−**d** have been carried out at the B3LYP/TZ2P and B3PW91/TZ2P levels, followed by harmonic frequency calculations at these levels. The relative energies and free energies at these levels, and also at the B3LYP/6-31G* level, are given in Table 2. Isomer **2b** is predicted to be the lowest in free energy.

Figures 1−4 of the Supporting Information show the B3PW91/TZ2P structures of the CC conformations of **2a**−**d**. Table 1 of the Supporting Information lists selected dihedral angles.

IR and VCD Spectroscopies. The IR and VCD spectra of a $CHCl_3$ solution of (+)-**2** have been measured in the mid-IR spectral region, 800−1600 cm^{-1} (Figure 5 of the Supporting Information). Analysis is carried out on the basis of the IR and VCD spectra predicted using DFT for the four isomers of **2**, **2a**−**d**. The IR and VCD

(15) Helgaker, T.; Jaszunski, M.; Ruud, K.; Górska, A. *Theor. Chim. Acta* **1998**, *99*, 175−182.
(16) Helgaker, T.; Watson, M.; Handy, N. C. *J. Chem. Phys.* **2000**, *113*, 9402−9409.
(17) Peralta, J. E.; Barone, V.; Scuseria, G. E.; Contreras, R. H. *J. Am. Chem. Soc.* **2004**, *126*, 7428−7429.
(18) de Castro, E. V. R.; Jorge, F. E. *J. Chem. Phys.* **1998**, *108*, 5225−5229.
(19) *NUTS*; Acorn NMR Inc.: Livermore, CA, www.acornnmr.com.
(20) Stephens, P. J.; McCann, D. M.; Devlin, F. J.; Cheeseman, J. R.; Frisch, M. J. *J. Am. Chem. Soc.* **2004**, *126*, 7514−7521.

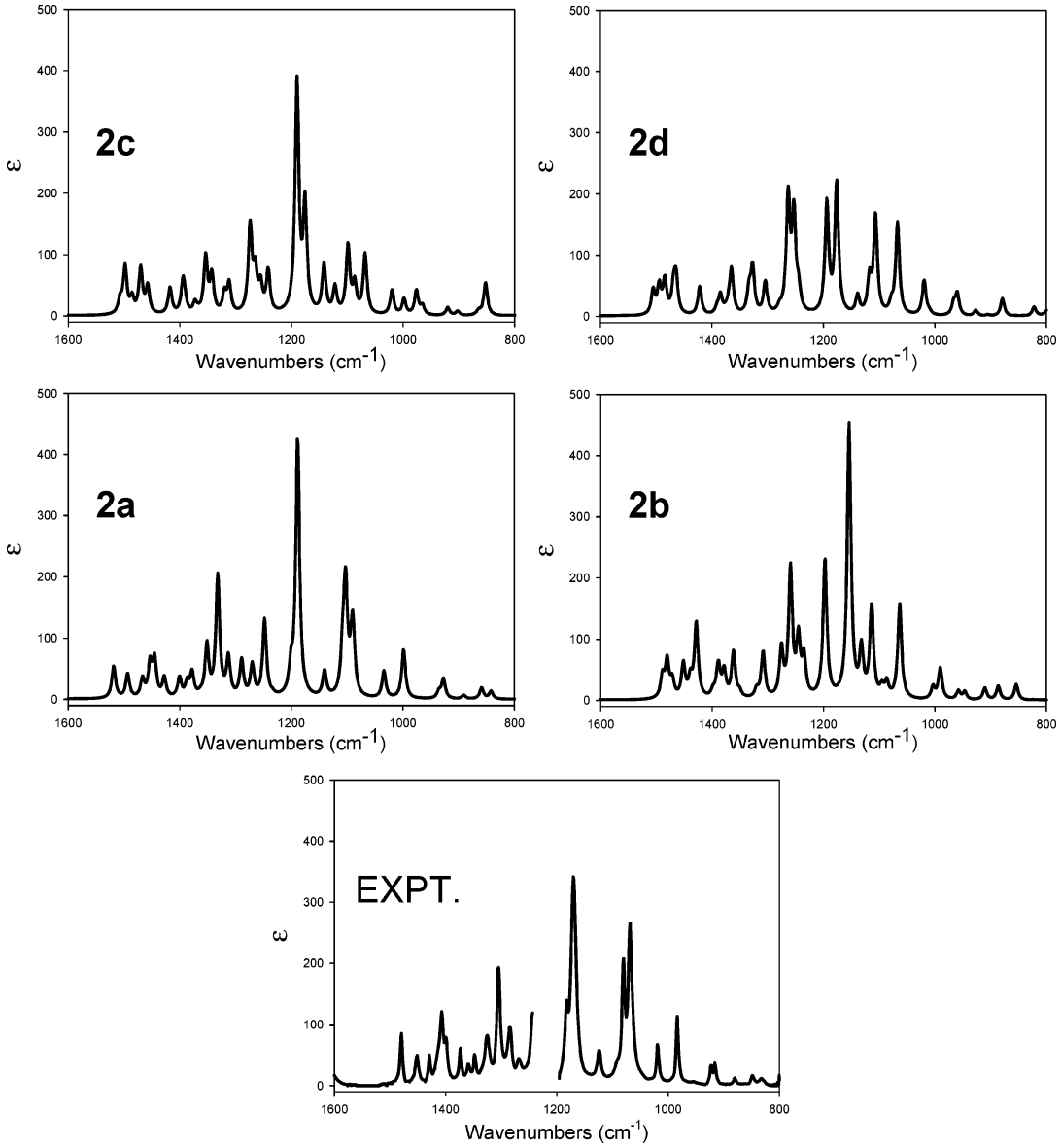

FIGURE 1. Comparison of the B3PW91/TZ2P IR spectra of **2a**−**d** to the experimental IR spectrum of (+)-**2** (from Figure 5 of the Supporting Information).

spectra of the CC conformations of (1*R*,6*R*)-**2a**, (1*R*,6*S*)-**2b**, (1*R*,6*S*)-**2c**, and (1*S*,6*R*)-**2d** have been calculated using DFT at the B3LYP/TZ2P and B3PW91/TZ2P levels. Calculated frequencies, dipole strengths, and rotational strengths are given in Tables 2−5 of the Supporting Information. IR and VCD spectra were synthesized thence using Lorentzian band shapes (γ = 4.0 cm^{-1}). Comparison of the B3PW91/TZ2P and B3LYP/TZ2P spectra to the experimental spectra shown in Figures 1 and 2 and in Supporting Information Figures 6 and 7, respectively, leads immediately to the conclusion that the isomer obtained synthetically is **2a**.

As seen in Figures 8 and 9 of the Supporting Information, the B3PW91/TZ2P IR and VCD spectra of **2a** are in slightly better agreement with the experimental spectra than are the B3LYP/TZ2P spectra. Detailed analysis of the experimental spectra is therefore based on the B3PW91/TZ2P calculations. The B3PW91/TZ2P IR spectrum of **2a** is compared to the experimental IR spectrum in Figure 3. Overall, the agreement is excellent and the assignment of the fundamental transitions in the experimental spectrum is straightforward, with the exception of modes 28−31, as shown in Figure 3. Lorentzian fitting of the experimental spectrum leads to the experimental frequencies and dipole strengths given in Table 2 of the Supporting Information. Comparison of these parameters to the predicted values is shown in Figure 10 of the Supporting Information.

The B3PW91/TZ2P VCD spectrum of (1*R*,6*R*)-**2a** is compared to the experimental VCD spectrum of (+)-**2** in Figure 4. As with the IR spectrum, agreement is excellent and the assignment of fundamentals is straightforward, including for modes 28−31, as shown in Figure 4. Lorentzian fitting of the experimental VCD spectrum leads to the experimental frequencies and rotational strengths given in Table 2 of the Supporting Information. Comparison of predicted and experimental rotational strengths is shown in Figure 10 of the Supporting Information.

The agreement between calculated and experimental frequencies, dipole strengths, and rotational

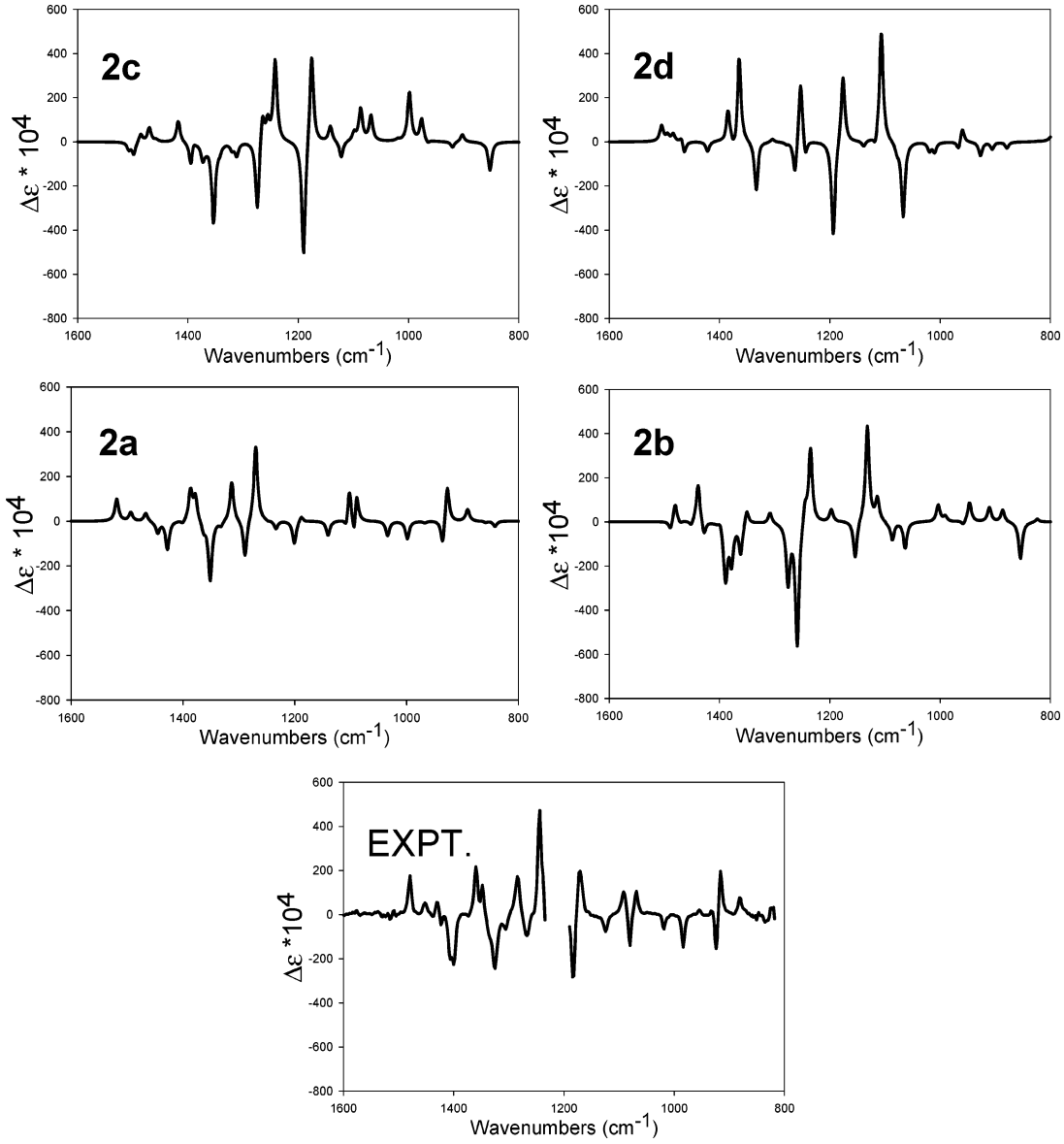

FIGURE 2. Comparison of the B3PW91/TZ2P VCD spectra of **2a**−**d** to the experimental VCD spectrum of (+)-**2** (from Figure 5 of the Supporting Information).

strengths is typical of DFT calculations using hybrid functionals and the TZ2P basis set[2c,d,3a,b,e−k] and unambiguously defines the structure of (+)-**2** as (1*R*,6*R*)-**2a**.

NMR. The ^{1}H, ^{13}C, DEPT-edited ^{13}C, HMQC, and COSY NMR spectra of a $CDCl_3$ solution of (±)-**2** have been measured. Figure 5 shows the gradient HMQC spectrum, together with the ^{1}H and ^{13}C spectra. ^{13}C resonances A−G are additionally labeled as methylene or methyne groups according to results from DEPT-edited ^{13}C spectra. Judging from its chemical shift and DEPT, resonance G is the CH_2 adjacent to the lactone ring oxygen. In the HMQC spectrum, methylene G correlates with the two proton resonances (protons 11 and 12) at δ 4.1, which is the chemical shift of a CH_2−OR group. These observations summarily rule out structure **2b** which contains a methyne group α to the lactone ring oxygen (CH−OR). Bridge-head hydrogens 8 and 10 differ substantially in chemical shift (δ 2.70 and 3.61, respectively) so H10 is closer to polar functionality. Geminal proton pairs are established by the HMQC spectrum as (1,4), (2,3), (5,6), (7,9), and (11,12). The observed coupling constants (Table 6 of the Supporting Information) confirm the geminal relationships of (1,4), (5,6), and (7,9); (2,3) and (11,12) are too second-order for geminal coupling to be seen.

The final answer with regard to the structure of **2** is given by the COSY spectrum in Figure 6. Each isomer, **2a**−**d**, possesses only one pair of vicinal methylenes (CH_2−CH_2). Structure **2a** is unique in having the CH_2 α to the lactone ring oxygen be one of the two vicinal methylenes. Off-diagonal correlation peaks in Figure 6 of resonances 1 and 4 with (11,12) establish (1,4) and (11,12) as the vicinal methylenes. Since (11,12) is also the methylene α to the lactone ring oxygen, the COSY spectrum is only consistent with structure **2a**.

The complete assignments of ^{1}H and ^{13}C atom resonances, largely from the DEPT, HMQC, and COSY spectra, are shown in Figure 7. Several other features of the COSY spectrum help in these assignments. Cross-

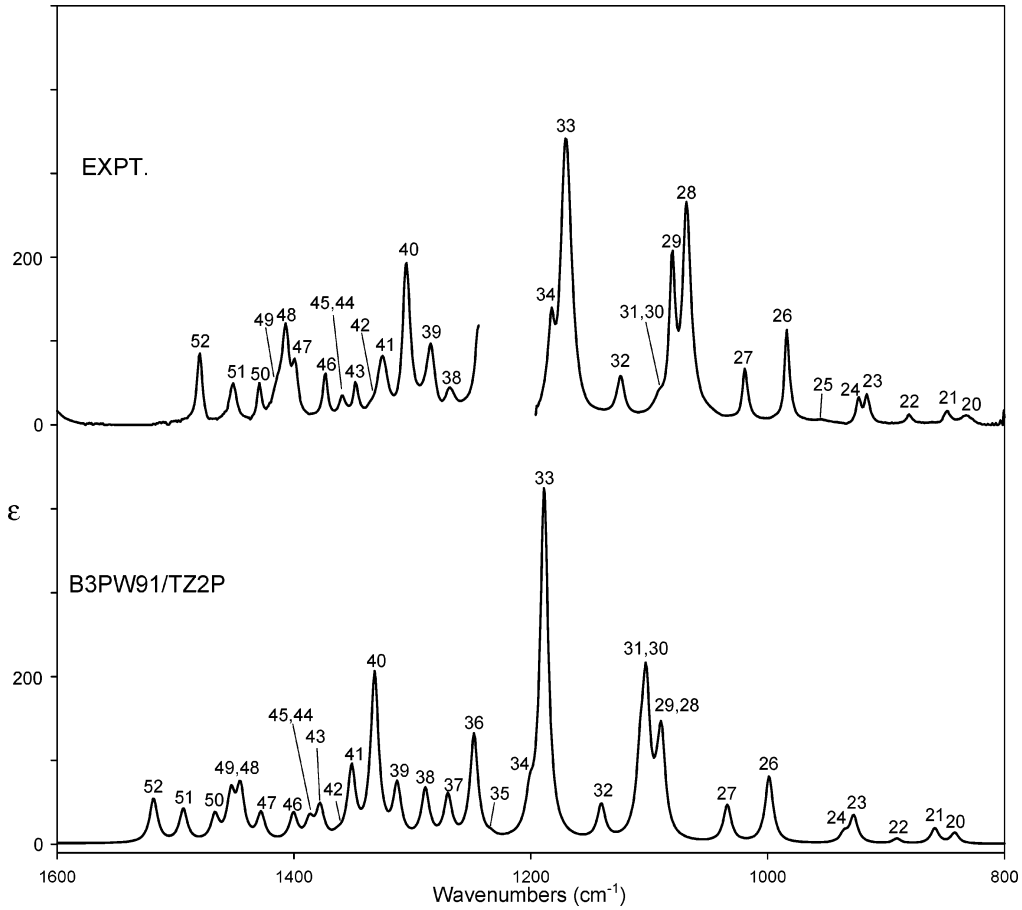

FIGURE 3. Assignment of the experimental IR spectrum of (+)-**2** using the B3PW91/TZ2P IR spectrum of **2a**. Fundamental transitions are numbered.

peaks of (2,3) with 8 and with 10 establish (2,3) as the methylene bridge, and the fact that 10 is at a lower field means that it is adjacent to the acyl carbon. It is interesting that (11,12) shows cross-peaks with (2,3), 7, and 9 (the last very weak). These are all six-bond couplings, so the ester group in this relatively rigid structure apparently effectively transmits the coupling. The vicinal coupling between 7 and 10 is strong as well which confirms that the (7,9) methylene is adjacent to methyne 10 and not methyne 8. While atom connectivities in **2a** are established by the HMQC and COSY spectra, their relative stereochemical arrangements are not. The stereochemical assignments in Figure 7 are derived from the DFT calculations we now discuss.

Further support for the above analysis is provided by DFT calculations of the ^{1}H and ^{13}C NMR spectra for **2a**−**d**. The calculated ^{1}H NMR spectra of **2a**−**d** (Figure 8 and Supporting Information Figures 12−14) vary substantially, particularly in the chemical shift range of δ 3−5. In particular, the spectrum of **2a** is the only one where resonances for three protons appear below δ 3.0, as in the experimental spectrum. As shown in Figure 8, the calculated spectrum of **2a** bears a strong resemblance to the experimental spectrum. The calculated spectra of **2b**−**d** are in much worse agreement, further supporting the identification of the experimental isomer as **2a**. The calculated proton chemical shifts and coupling constants of **2a** are listed in Table 7 of the Supporting Information. The calculated and experimental chemical shifts are compared in Figure 9. Note that the order of chemical shifts of protons 6 and 7 is reversed from the calculated to the experimental spectra. The discernible experimental J_{HH} values are also compared to the corresponding calculated values in Figure 9.

The four calculated ^{13}C spectra (Figure 15 of the Supporting Information) are all quite similar and do not discriminate between the isomers **2a**−**d**. The calculated ^{13}C chemical shifts of **2a** are compared to the experimental shifts in Figure 9.

Optical Rotation and Electronic Circular Dichroism. We have calculated the specific rotation of the CC conformation of (1*R*,6*R*)-**2a** using the TDDFT/GIAO methodology. The functional and basis set are B3LYP and aug-cc-pVDZ, respectively; the geometry is B3LYP/6-31G*. The results for five wavelengths from 589.3 to 365 nm are compared to experimental values for a $CHCl_3$ solution of (+)-**2** in Table 3. Both calculated and experimental specific rotations increase monotonically with decreasing wavelength. At all wavelengths, the predicted rotation is opposite in sign to the measured rotation.

The electronic circular dichroism (ECD) of (+)-**2** has been reported by Stončius, Berg, and Butkus.[5] We have calculated the electronic excitation energies and rotational strengths of the CC conformation of (1*R*,6*R*)-**2a**, again using the TDDFT methodology with B3LYP and aug-cc-pVDZ at the B3LYP/6-31G* geometry. The results are given in Table 4, and compared to the experimental ECD spectrum in Figure 10. The two lowest excitations

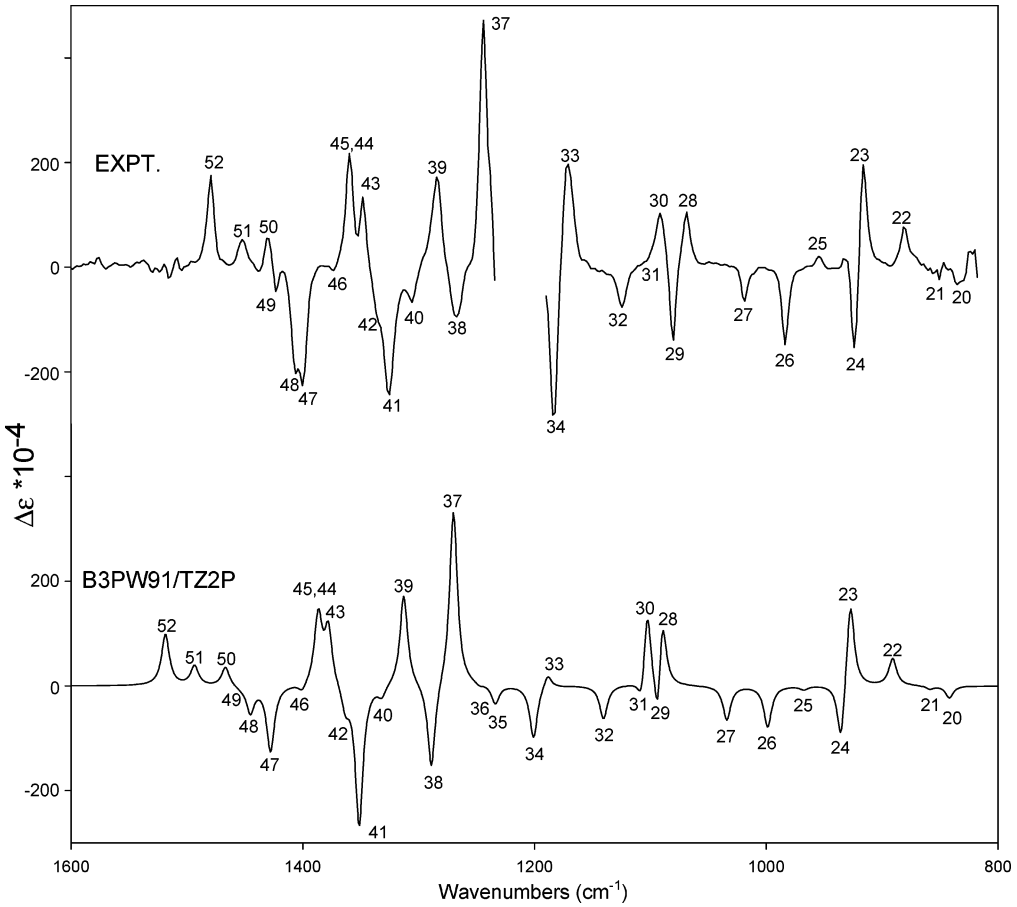

FIGURE 4. Assignment of the experimental VCD spectrum of (+)-**2** using the B3PW91/TZ2P VCD spectrum of (1*R*,6*R*)-**2a**. Fundamental transitions are numbered.

are predicted at 299 and 233 nm, in excellent agreement with the observed bands at 298 and 228 nm. These excitations are attributable to the n → π^* excitations of the ketone and lactone groups, respectively. With respect to the signs and magnitudes of the rotational strengths of these two excitations, agreement is less good. The signs of the rotational strengths of the ketone and lactone n → π^* transitions are incorrect and correct, respectively. For the lactone n → π^* excitation, the calculated rotational strength is much smaller than the experimental value (Table 4). Thus, the TDDFT/GIAO calculations are in poor agreement with experiment for both the optical rotation and the ECD of **2**.

We have also calculated the specific rotation and ECD of the lowest-energy conformations of (1*R*,6*S*)-**2b**, (1*R*,6*S*)-**2c**, and (1*S*,6*R*)-**2d**, with the results given in Table 8 of the Supporting Information.

The dependence of the predicted specific rotation and the ECD of the CC conformation of (+)-**2a** on the functional, basis set, and equilibrium geometry has been explored. Changing the functional to B3PW91 or the basis set to 6-311++G(2d,2p) leads to very minor changes in $[\alpha]_D$, $[\alpha]_{546}$, and the rotational strengths of the two lowest excitations (Table 9 of the Supporting Information). On the other hand, substantial variation in $[\alpha]_D$ and $[\alpha]_{546}$ occurs on changing the equilibrium geometry. Over 8 different ab initio geometries, $[\alpha]_D$ varies from −18.0 to −82.7. Using AM1 and MMFF94 geometries, $[\alpha]_D$ is −77.9 and −129.7, respectively. A plot of $[\alpha]_D$ against the dihedral angle C1−C2−O3−C4, Figure 11, shows a regular variation, with $[\alpha]_D$ becoming increasingly/decreasingly negative as the C1−C2−O3−C4 angle increases/decreases. At the B3PW91/TZ2P geometry, which has the smallest C1−C2−O3−C4 angle 12.2°, $[\alpha]_D$ is −18.0, as compared to the value of −43.8° for the B3LYP/6-31G* geometry where the angle is 17.2°. If the lactone group is constrained to be planar (C1−C2−O3−C4 = 0°), B3LYP/6-31G* and B3PW91/TZ2P geometries lead to positive $[\alpha]_D$ values of +21.6 and +26.1, respectively. At the same time, however, minor variation in electronic rotational strengths is observed: the ranges for the carbonyl and lactone n → π^* transitions are −1.7 to −0.9 and 11.6 to 16.5, respectively, over the set of ab initio geometries. Thus, the poor agreement of calculated and experimental specific rotations and ECD spectra cannot simultaneously be accounted for by assuming that the nonplanarity of the lactone group is incorrectly predicted.

Discussion

TDDFT calculations have, to date, been quite successful in predicting the transparent spectral region optical rotations and ECD spectra of chiral organic molecules.[6,7,20] It was therefore surprising to us to find that the calculations for the keto-lactone **2a** were in very poor agreement with the experimental data for the Baeyer−Villiger oxidation product of the dione **1**, which had been identi-

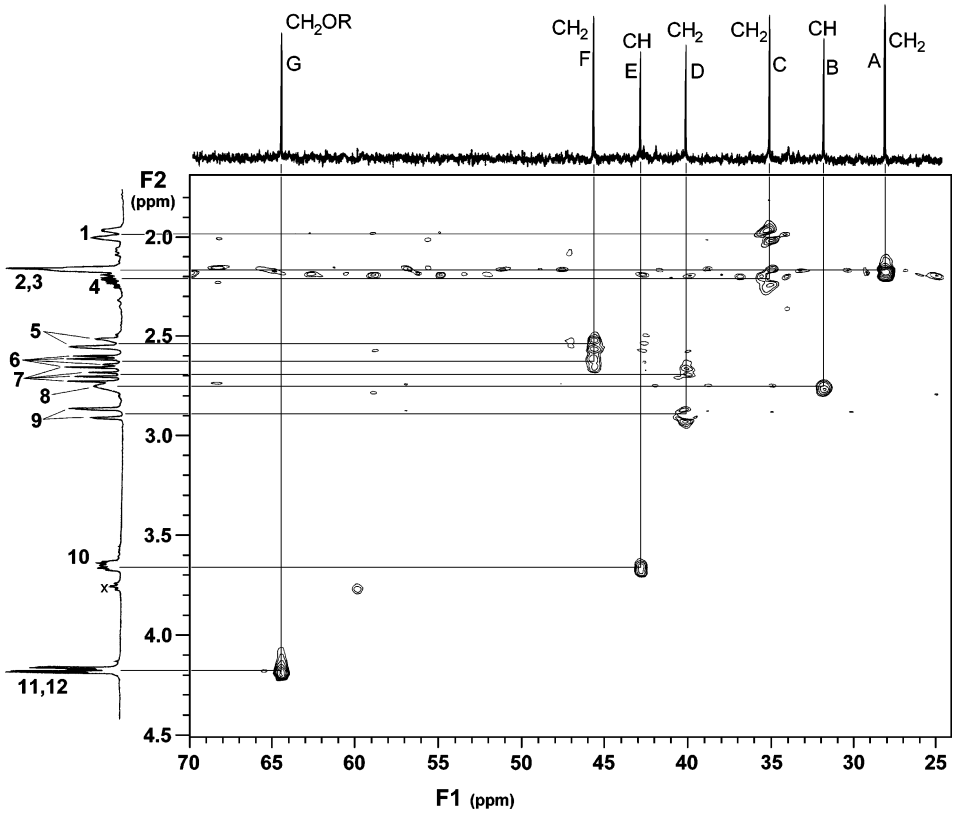

FIGURE 5. gHMQC (pulsed *z*-gradient, inverse-detected, $^{1}H-^{13}C$ correlation) spectrum of **2**. The assignments shown above the carbon resonances are from the DEPT spectra.

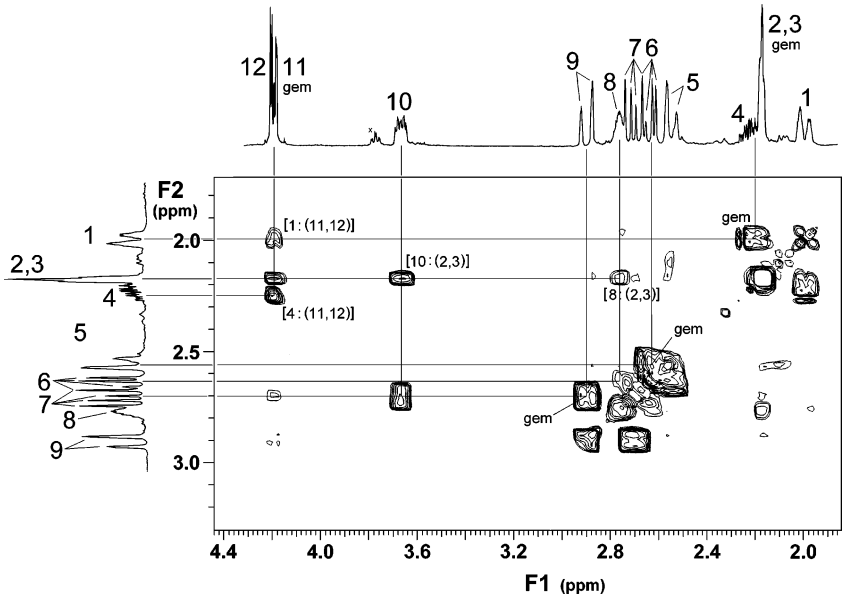

FIGURE 6. Pulsed *z*-gradient COSY (gCOSY) of **2**.

fied as **2a** by ^{1}H NMR spectroscopy. An obvious possibility for the discrepancies in OR and ECD was that the keto-lactone is not **2a** but one of the isomers, **2b**−**d**. Application of the standard rules for the relative migratory aptitudes of the groups adjacent to the ketone leads to the expectation that **2b** would be the preferred product. In addition, DFT calculations (Table 2) predict that **2b** is the isomer of lowest free energy and, hence, the thermodynamically preferred product. It therefore became important to re-examine the structure of **2**.

The IR and VCD spectra of a chiral molecule are sensitive functions of its stereochemistry and, in the case of VCD, of its chirality. We have exploited this sensitivity to study both the conformational structures and the ACs of a number of chiral molecules.[3a−k] It is a natural extension of this work to apply IR and VCD spec-

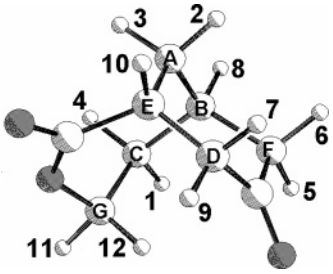

FIGURE 7. Assignments of experimental ^{1}H and ^{13}C resonances.

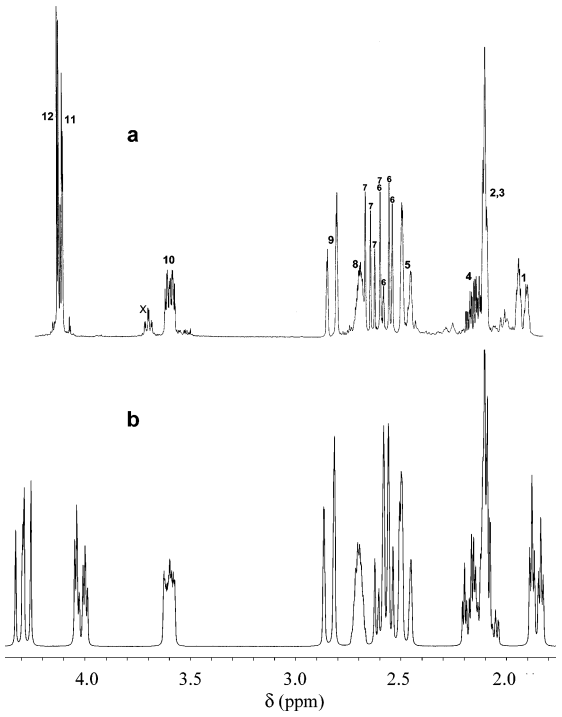

FIGURE 8. (a) Experimental ^{1}H NMR spectrum of **2** and (b) calculated ^{1}H NMR spectrum of the CC conformation of **2a**.

troscopies to the discrimination of stereoisomers. Accordingly, we have applied these techniques to characterize the structure of the Baeyer−Villiger oxidation product of **1**. Conformational analysis of the four possible ketolactone products, **2a**−**d**, using DFT at the B3LYP/6-31G* level predicts in each case that the conformation of lowest free energy is the CC conformation and that at equilibrium at room temperature the CC population is >95%. As a result, higher-energy conformations can be ignored. IR and VCD spectra of the CC conformations of **2a**−**d** have been predicted via DFT using a large basis set (TZ2P) and two state-of-the-art hybrid functionals (B3LYP and B3PW91). The predicted IR and VCD spectra of the four isomers of **2a**−**d** vary greatly. As a result, a comparison of the calculated spectra to the experimental spectra in the mid-IR spectral region immediately defines the isomer obtained experimentally. Qualitatively, the agreement of the calculated spectra for **2a** with the experimental spectra is excellent allowing immediate assignment of the experimental spectra. For **2b**−**d**, the calculated spectra do not resemble the experimental spectra and do not permit convincing assignment of the latter. It follows that **2a** is the isomer obtained experimentally from **1**. The comparison of the calculated VCD spectrum of (1*R*,6*R*)-**2a** to the experimental VCD spectrum of (+)-**2** further confirms that the AC of (+)-**2a** is 1*R*,6*R*. Subsequently, we have revisited the ^{1}H and ^{13}C NMR spectra of **2**, both experimentally and theoretically.

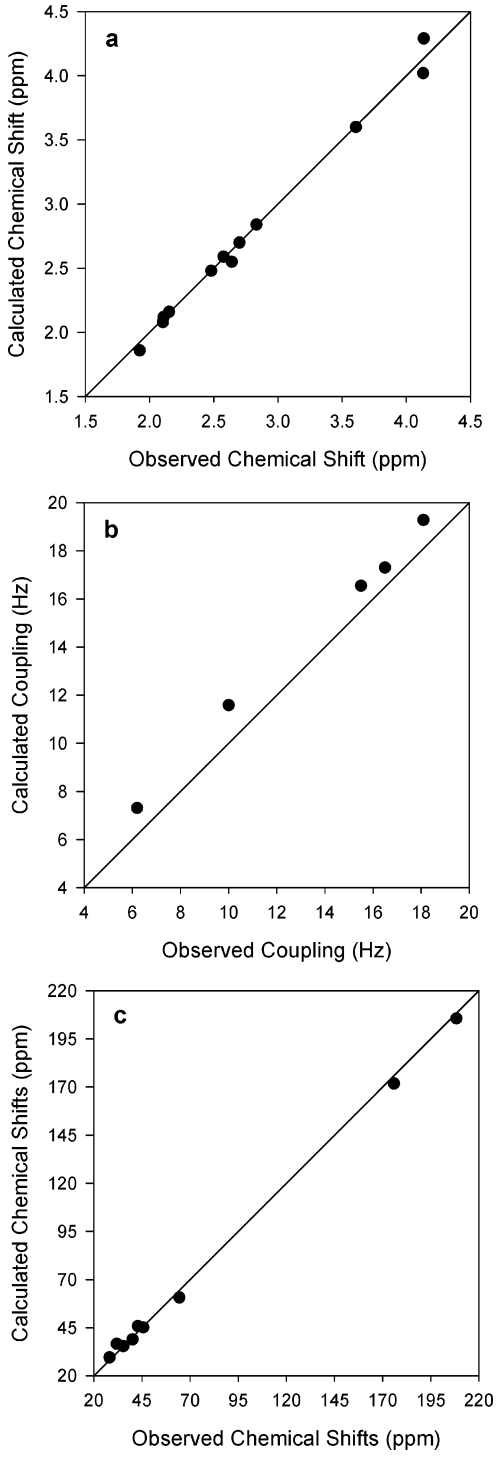

FIGURE 9. (a) Comparison of calculated ^{1}H chemical shifts of the CC conformation of **2a** with the experimental chemical shifts of **2**. (b) Comparison of calculated coupling constants, J_{HH}, of the CC conformation of **2a** with the experimental coupling constants of **2**. (c) Comparison of calculated ^{13}C chemical shifts of the CC conformation of **2a** with the experimental chemical shifts of **2**. The lines all have a slope of +1.

TABLE 3. Experimental Specific Rotations of (+)-2 and Calculated Specific Rotations of (1*R*,6*R*)-2a

λ (nm)	expt[a]	calcd[b]
589.3	13.0	−43.8
578	13.9	−45.9
546	16.5	−52.6
436	35.5	−94.5
365	77.9	−174.9

[a] $c = 1.0$ (0.061 M) in $CHCl_3$. [b] B3LYP/aug-cc-pVDZ//B3LYP/6-31G*.

TABLE 4. Calculated and Experimental Electronic Excitation Energies and Rotational Strengths

calcd[a]				expt[b]			
Δ*E* (eV)	λ(nm)	R_{vel}[c]	R_{length}[c]	Δ*E* (eV)	λ (nm)	R_{expt}[c,d]	Δε
4.15	299	−1.2	−1.3	4.15	298	3.0	1.1
5.32	233	12.5	12.2	5.44	228	66.3	18.6
5.55	223	−1.2	−1.4				
5.76	215	−9.8	−9.7				
6.03	206	−2.2	−2.1				
6.27	198	−0.9	−0.9				
6.35	195	6.5	6.6				
6.40	194	0.3	0.2				

[a] (1*R*,6*R*)-**2a** in the CC conformation. [b] (+)-**2** in 95% aqueous EtOH. [c] In 10^{-40} esu^2 cm^2. [d] Obtained by integration over the ranges 201−260 and 280−320 nm.

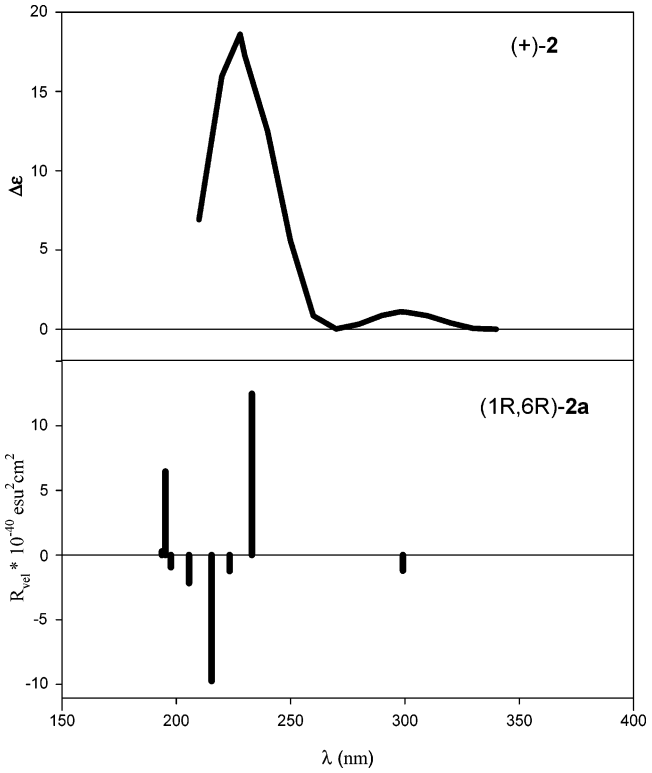

FIGURE 10. Experimental ECD of (+)-**2** and calculated ECD of the CC conformation of (1*R*,6*R*)-**2a**.

Analysis of the HMQC, COSY, and DEPT-edited ^{13}C spectra of **2** and comparison of ^{1}H and ^{13}C spectra predicted using DFT for **2a**−**d** to the experimental spectra both lead to the conclusion that only isomer **2a** is consistent with the experimental spectra, confirming the conclusion arrived at using IR and VCD spectroscopies. In sum, the product of Baeyer−Villiger oxidation of (+)-**1** is unambiguously (+)-**2a**, as reported by Butkus and Stončius,[4] and not **2b**, as expected from mechanistic considerations. The regioselective formation of **2a** could be due to electronic factors, since the carbonyl group at C2 of **1** might significantly reduce the migratory aptitude of the neighboring bridge-head carbon. Further investigation, both experimentally and computationally, of the mechanism of this reaction to elucidate the factors responsible for the formation of **2a** from **1** is desirable.

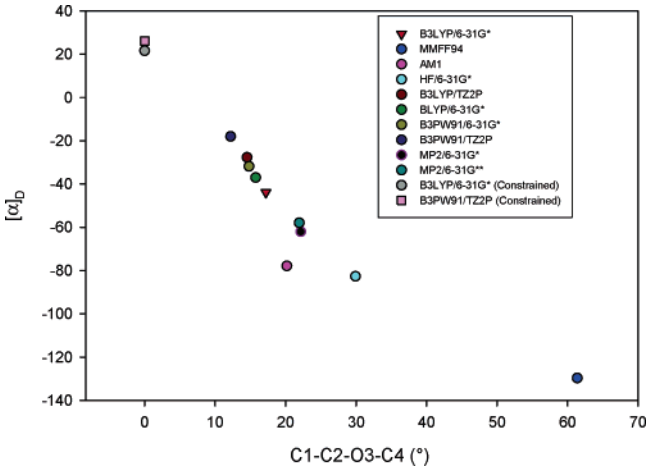

FIGURE 11. Variation of calculated $[\alpha]_D$ for the CC conformation of (1*R*,6*R*)-**2a** with the C1−C2−O3−C4 dihedral angle.

Since the Baeyer−Villiger oxidation product of (+)-(1*R*,5*S*)-**1** is indeed (+)-(1*R*,6*R*)-**2a**, we must accept that the TDDFT calculations for the specific rotation and ECD spectrum of **2a** are substantially inaccurate. In particular, the determination of the AC of **2a** via the specific rotation or the ECD of the ketone n → π* transition leads to an incorrect result. At the time when this was discovered, it was the first case known to us where the TDDFT specific rotation was of the wrong sign. Subsequently, we have identified several more molecules (two alkanes, one alkene, and three ketones, all with $[\alpha]_D$ values < 100) for which calculated specific rotations are incorrect in sign.[21] The keto-lactone **2a** is, therefore, not unique in this regard. These results show that the determination of ACs of chiral molecules via TDDFT calculations of their specific rotations is not 100% reliable when the rotations are small. Over a set of 65 molecules, having experimental $[\alpha]_D$ values < 100, the RMS error (σ) of B3LYP/aug-cc-pVDZ//B3LYP/6-31G* calculated $[\alpha]_D$ values was 28.9. In the case of **2a**, the deviation of the calculated $[\alpha]_D$ value for this functional, basis set, and geometry is 56.8, approximately equal to the 2σ deviation for the 65-molecule set. Further TDDFT calculations of the specific rotations and ECD spectra of lactones and keto-lactones are in progress to further define their statistical accuracy for molecules containing these functional groups. In the meantime, the case of **2a** shows that the determination of ACs from specific rotations is not "simple and reliable"[22] and constitutes a cautionary tale for those making use of TDDFT calculations of specific rotations to determine ACs.

(21) Stephens, P. J.; McCann, D. M.; Cheeseman, J. R.; Frisch, M. J. *Chirality* **2005**, *17*, S52−S64.
(22) Giorgio, E.; Viglione, R. G.; Zanasi, R.; Rosini, C. *J. Am. Chem. Soc.* **2004**, *126*, 12968−12976.

Finally, we note the excellent agreement of calculated ^{1}H and ^{13}C chemical shifts and $^{1}H-^{1}H$ coupling constants for **2a** with experiment, demonstrating the reliability of the DFT methodology used, including the specific choices of basis set, in predicting these parameters. While this is not surprising for the chemical shifts,[23] the accuracy of the spin−spin coupling constants was less predictable. Our results suggest that the DFT prediction of NMR spectra, including the effects of spin−spin coupling, is now a practical methodology for the structural analysis of organic molecules via their NMR spectra.

Conclusion

We have presented the first example of the use of VCD spectroscopy to differentiate between structural isomers of a chiral molecule. Our conclusions were supported by NMR spectroscopy. For the majority of molecules, NMR undoubtedly provides the most efficient spectroscopic method for the discrimination of structural isomers. Our work here simply shows that this can also be achieved via IR and VCD spectroscopies combined with DFT calculations. In those specific cases where NMR analysis is not straightforward, these techniques can therefore offer a practical alternative.

Acknowledgment. We acknowledge financial support of this research by the National Science Foundation (Grant CHE-0209957 to P.J.S.) and the Lithuanian Science and Studies Foundation (Grant C-02/2003 to E.B.). We are also grateful to the USC Center for High Performance Computing for computer time.

(23) (a) Magyarfalvi, G.; Pulay, P. *J. Chem. Phys.* **2003**, *119*, 1350−1357. (b) Rablen, P. R.; Pearlmann, S. A.; Finkbiner, J. *J. Phys. Chem. A* **1999**, *103*, 7357−7363.

Supporting Information Available: B3PW91/TZ2P structures of **2a**−**d**; dihedral angles of the CC conformations of **2a**−**d**; experimental IR and VCD spectra of (+)-**2** in $CHCl_3$; comparisons of the calculated frequencies, dipole strengths, and rotational strengths for the CC conformation of (1*R*,6*R*)-**2a** to experimental values for **2**; calculated frequencies, dipole strengths, and rotational strengths for the CC conformations of **2b**−**d**; comparisons of the B3LYP/TZ2P IR and VCD spectra of **2a**−**d** to the experimental IR and VCD spectra of (+)-**2**; comparison of the B3PW91/TZ2P and B3LYP/TZ2P IR and VCD spectra of (1*R*,6*R*)-**2a** to the experimental IR and VCD spectra of (+)-**2**; comparison of B3PW91/TZ2P and B3LYP/TZ2P frequencies, dipole strengths, and rotational strengths for (1*R*,6*R*)-**2a** to the experimental parameters for (+)-**2**; observed chemical shifts and coupling constants of **2**; calculated ^{1}H NMR spectra for **2b**−**d**; calculated ^{1}H chemical shifts and coupling constants for **2a**; calculated ^{13}C NMR chemical shifts of **2a**−**d** compared with the experimental ^{13}C spectrum of **2**; calculated excitation energies and rotational strengths for **2b**−**d**; variation of specific rotations, excitation energies, and rotational strengths of (1*R*,6*R*)-**2a** with the functional, basis set, and geometry; Cartesian coordinates of B3LYP/6-31G*, B3LYP/TZ2P, and B3PW91/TZ2P optimized geometries of molecules **2a**−**d**. This material is available free of charge via the Internet at http://pubs.acs.org.

JO047906Y